RSC Advances

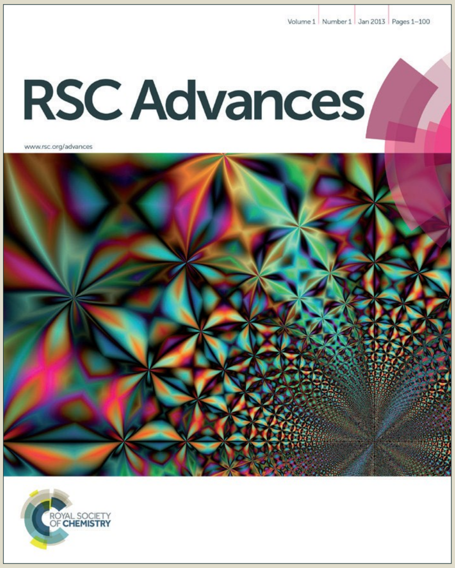

ROYAL SOCIETY OF CHEMISTRY

www.rsc.org/advances

Novel hybrid epoxy silicone materials as efficient anticorrosive coatings for mild steel

Rami Suleiman[a,]*, Hatim Dafalla[b], Bassam El Ali[c]

[a] *Center of Research Excellence in Corrosion (CoRE-C), King Fahd University of Petroleum & Minerals (KFUPM), Dhahran 31261, Saudi Arabia, E-mail:* *ramismob@kfupm.edu.sa*
[b] *Center for Engineering Research, King Fahd University of Petroleum & Minerals (KFUPM), Dhahran 31261, Saudi Arabia*
[c] *Chemistry Department, King Fahd University of Petroleum & Minerals (KFUPM), Dhahran 31261, Saudi Arabia*

Abstract

Novel hybrid-sol-gel materials (C1-C5) based on silica-epoxy composite resins were successfully prepared by coupling different aminosilanes with DER736 epoxy resin, followed by in situ sol-gel process, and finally introducing the urethane moieties to the final coatings. The research has emphasized on the effect of changing the type of the aminosilane on the properties of the prepared hybrid coatings. Three different aminosilanes were examined and their reaction parameters with the epoxy and the trialkoxysilanes were carefully optimized in order to avoid fast gelation and to obtain the desired properties of the hybrid coatings. The prepared organic-inorganic hybrid coatings were loaded and cured on mild steel panels and characterized for FTIR, NMR, TGA, water contact angles (WCA), nanoindentation hardness, pull-off adhesion, SEM, EIS and polarization studies. The results revealed that the coatings prepared from the trialkoxysilanes APTMS and MTMS (C4) demonstrate the best mechanical, anticorrosion and adhesion properties on mild steel substrate as compared to all other coatings in 3.5 wt% NaCl medium. Electrochemical impedance spectroscopy (EIS) results indicated a corrosion resistance value for this coating in the range of 10^6 Ω cm^2 after 10 days of continuous immersion in the saline medium. The SEM observations suggest that coatings produced from the other aminosilanes, APT-PDMS and APM-DMS are inhomogeneous and having some defects which had ultimately affected their barrier protection properties.

Keywords:
Hybrid; Mild steel; Corrosion; Impedance Spectroscopy; Epoxy; Coatings.

---

* Corresponding authors. Tel.: +966-3-8607580. Fax: +966-3-8603996.

INTRODUCTION

The total cost and environmental consequences of the corrosion problems of the metal surfaces have become a major challenge to many industries, especially for the gas and oil industry.[1] Mild steel is used in large tonnages in marine applications, nuclear power and fossil fuel power plants, transportation, chemical processing, petroleum production and refining, pipelines, mining, construction and metal-processing equipment. Mild steels are vulnerable to very high corrosion rates in aggressive solutions and atmospheres due to their nature of limited alloying content.[2] Protective coatings are typically employed to protect the steel surface from corrosion. Chromate-based corrosion inhibitors have been used extensively in corrosion resistant coatings. However, the hexavalent chromium Cr(VI) ingredient is highly carcinogenic and is on the way of being abandoned. Thus, current researches on coatings are targeting to produce environmental friendly alternatives with equivalent or enhanced corrosion protection.[3]

In the last two decades, the potential of hybrid organic-inorganic sol-gel materials for the replacement of chrome conversion treatments has been the topic of a huge number of studies.[4-7] These materials combine the balanced properties of organic polymers (e.g., flexibility, ductility, dielectric) and silica (e.g., high thermal stability, strength, hardness, UV-VIS absorbance), thus having interesting mechanical and barrier properties on metal surfaces.[8-10] Sol-gel derived organic-inorganic hybrid coatings are mainly produced through the hydrolysis and condensation reaction of organofunctional alkoxysilane precursors.[11, 12] They were prepared also by the blending of siloxanes with hydrocarbon-based polymers; more notably epoxy resins.[13, 14] The corrosion resistance of these coatings has been attributed to their physical barrier properties, which restrict the penetration of the electrolyte towards the metallic substrate.[15] The chemical structure and organic functionality of silanes can be varied and optimized in order to achieve the maximum effect in terms of hydrolytic stability of the interface, desired hydrophobicity or adhesion properties. Coating's formulator should avoid phase separation between the soft (organic) and hard (inorganic) components of the hybrid system. A general approach to increase the crosslink density and thus obtain strong interfacial interactions between the organic and inorganic components is to use silica coupling agents. The functional group present in the crosslinker establishes a bridge between the two components; thus well-dispersed nanostructured phases may result.[16] Many siliconized epoxy hybrid materials were prepared using the above methodology and reported in literature,[17-20] However, reports on similar materials having urethane moieties are very rare.[21] The production of such novel hybrid sol-gel materials of superior mechanical and barrier properties is still a very challenging area for research.

In this study, we have prepared successfully a series of novel siliconized-epoxy hybrid sol-gel materials via the blending of aminosilane derivatives with the epoxy resin DER736, followed by the hydrolysis/polycondensation of the existing silanol groups, and finally the conversion of the unreacted -OH groups into urethane moieties in the final coatings. The target is to prepare hybrid coatings that are having the advantage of combining silane, epoxy and urethane properties in a single system, and to study the effect of the type of the aminosilane crosslinking agent on the coating properties. Three different aminosilanes were tested during the preparation of coatings which ultimately demonstrated to have major effect on the mechanical, anticorrosion and adhesion properties for the new coatings. Full spectral (FTIR, NMR), surface (SEM, contact angle), mechanical (TGA, hardness) and electrochemical (EIS, polarization) characterizations were conducted on the new coatings in order to evaluate their performance as protective coatings for mild steel substrates against corrosion.

EXPERIMENTAL

Materials

Tetraethoxysilane (TEOS), methyltrimethoxysilane (MTMS), 3-glycidoxypropyltrimethoxysilane (GPTMS), (3-aminopropyl)trimethoxysilane (APTMS), diglycidyl ether of polyoxypropylene glycol (DER736), isophorone diisocyanate (IPDI) and isopropyl alcohol (IPA) were purchased from Sigma-Aldrich (US). Aminopropyl terminated polydimethylsiloxane (Mwt= 5000) (APT-PDMS) was purchased from Flurochem (UK). 6-7%-Aminopropylmethylsiloxane-dimethylsiloxane copolymer (APM-DMS) was purchased from Gelest Inc. (US). All of the above chemicals were used as received and their chemical structures are given in the supporting information. Nitric acid (HNO_3) and sodium chloride (NaCl) was purchased from Loba Chemie, India. All reagents (HNO_3 and NaCl) used for the study were analar grade and deionized water was used for their preparation.

Preparation of the hybrid coatings

The preparation of the hybrid coatings involves three steps: the coupling reaction between the epoxy groups in DER736 and the amino groups in the aminosilanes, the reaction of the silanol groups in the alkoxysilanes that undergo hydrolysis and polycondensation reactions forming the inorganic polymeric network, and the reaction of the isocyanate groups in IPDI with the remained unreacted -OH groups in the hybrid polymer forming the urethane moieties. The order of the above steps and the amount of reactants was tuned carefully during the preparation of coatings in order to control the fast gelation and to deal with the poor mechanical properties of the final hybrid coatings. Initial coatings prepared without adding the IPDI were observed to have bad mechanical properties and low aging stability. Coating C2, in particular, required the silane precursor GPTMS in its composition to gain extra aging stability. In some experiments, IPA has to be added to the reaction mixture in order to slow the release of water to the silane mixture and thus inducing more control on the hydrolysis/polycondensation reactions. Direct mixing of the amine crosslinker, DER736 and IPDI produced coatings that wouldn't completely cure even after long drying in oven at high temperatures. Table 1 summarizes the details on the preparation of the hybrid coatings (C1-C5) that showed promising stability, adhesion and mechanical properties.

Table 1. Composition of the prepared hybrid coatings

Sample Code*	Composition (volume in mL)					Order of mixing (At room temp.)
	Silane	Aminosilane	Epoxide	IPDI	IPA	
C1	TEOS (10)	APT-PDMS (5)	DER736 (2)	2	-	Mix APT-PDMS with TEOS and DER736 for 3 hours. Add 1 mL of (0.05N HNO_3: IPA) and mix for overnight. Add IPDI and mix continuously.
C2	GPTMS (5) + MTMS (10)	APM-DMS (5)	DER736 (2)	2	-	Mix APM-DMS with GPTMS for 1 hour. Add MTMS and mix for 1 hour. Add 1 mL of (0.05N HNO_3: IPA) and mix for overnight. Add DER736 and mix for 3 days. Add IPDI and mix continuously.
C3	TEOS (10)	APT-PDMS (5)	DER736 (2)	4	10	Mix APT-PDMS with TEOS, DER736 and IPA for overnight. Add 0.5 mL of (0.05N HNO_3: IPA) and mix for overnight. Add IPDI and mix continuously.
C4	MTMS (10)	APTMS (5)	DER736 (2)	4	-	Mix APTMS with MTMS for 1 hour. Add DER736 and mix for 4 hours. Add 1 mL of (0.05N HNO_3: IPA) and mix for overnight. Add 4 IPDI and mix continuously.
C5	MTMS (10)	APT-PDMS (5)	DER736 (2)	4	10	Mix APT-PDMS with MTMS, DER736 and IPA for overnight. Add 1.0 mL of (0.05N HNO_3: IPA) and mix for overnight. Add IPDI and mix continuously.

Coating Procedure

The newly-prepared coatings were applied on S-36 mild steel Q-panels (Q-Lab Company, US) using K101 rod coating applicator. The coated sample dried for an hour and then cured at 100 °C for 48 hours in oven. Q-panel sheets had been cleaned ultrasonically for 10 minutes in absolute ethanol and air-dried prior to the coating step.

Characterization

^{1}H and ^{13}C NMR spectra were recorded on 500 MHz Joel 1500 NMR machine. Chemical shifts (d) were reported in ppm relative to tetramethyl silane (TMS) using $CDCl_3$. The FTIR spectra for the hybrid coatings were collected in transmittance mode within 4000 to 400 cm^{-1} range at 64 scans using a Nicolet 6700 Fourier Transform (FT) Spectrometer (Thermo Electron Corporation, UK) equipped with a DTGS KBr detector. The thermal behavior of the synthesized hybrid sol-gel coatings was studied by thermogravimetry (TG) (Perkin-Elmer TGA 7, US) analysis at a heating rate of 10 °C min^{-1} through to 700 °C under nitrogen atmosphere.

The polarization studies were carried out using the GAMRY3000 corrosion measurement system. The potential of the electrode was varied from -0.25 V to 0.25 V, which is very close to the corrosion potential (E_{corr}) of mild steel substrate. The electrochemical cell used for the current study consists of the prepared coated electrode as the working electrode, a graphite rod as the counter electrode, a SCE as the reference electrode, and 3.5% sodium chloride as the electrolyte. Surface Masks (GAMRY) of area of 1 cm^2 was used to mask the analyzed surface. EIS data were collected using a GAMRY3000 potentiostat with a frequency range between 100 kHz – 10 mHz (100000 – 0.01 Hz). The number of points taken was 10/decade with AC Voltage of 10 mV.

The morphology of the coatings and cross sections before and after corrosion testing were studied using a JEOL JSM6610LV SEM. The contact Angle Measurement (CAM) Instrument DSA30 (KRUSS, Deutsch, Germany) was used to evaluate the aqueous contact angle (θw) by pendant drop method, and the results presented in this study were the mean values of three measurements collected from three different steel panels coated with the same individual coating.

The nanoindentation on the hybrid coatings were performed using a nanoindenter instrument (Model CSM Instruments NHT) fitted with a Rockwell diamond indenter having 100 μm tip radius at a final load of 50 mN. Hardness values were determined from the unloading part of the force–depth (F–d) curve. The evaluation of the adhesion strength of all hybrid coatings on mild steel panels was carried out using a Hydraulic Adhesion Tester from paint test equipment, UK.

RESULTS AND DISCUSSION

The network formation in the hybrid coatings takes place from the reaction of the amine groups of the crosslinker with the epoxy group of the DER736 followed by the Si-O-Si bond formation by acidic water. The prepared coatings are proposed to adhere to the steel surface via a bond formation between the unreacted Si-OH groups and the –OH groups on the metal. The formation of the hybrid network is a complicated chemical process, where network structure is being determined by the relative rates of formation of the organic and inorganic parts and the linkages between them.[22] Therefore, understanding the nature of chemical reactions occurred during the sol-gel processing and network growth is highly required for optimizing the synergy between the two components and ultimately the coating properties. Spectral characterizations play a great role in achieving this goal by providing valuable information that can be used to analyze the structure-property relationships and also comparing material properties.

Spectral Characterization

The proposed chemical structures of the new siliconized epoxy hybrid materials were confirmed using FTIR and NMR spectral techniques. No single chemical structure can be drawn for any of the prepared coatings since the presence of a variety of highly reactive -OH, -NH and -NCO groups can lead to many competitive reactions. However, following the disappearance and the appearance of new functionalities using the above-mentioned techniques gave insight on the occurrence of chemical reactions that led to the formation of the final hybrid coatings. As an example, a proposed chemical structure of the coating C4 is given in Figure 1.

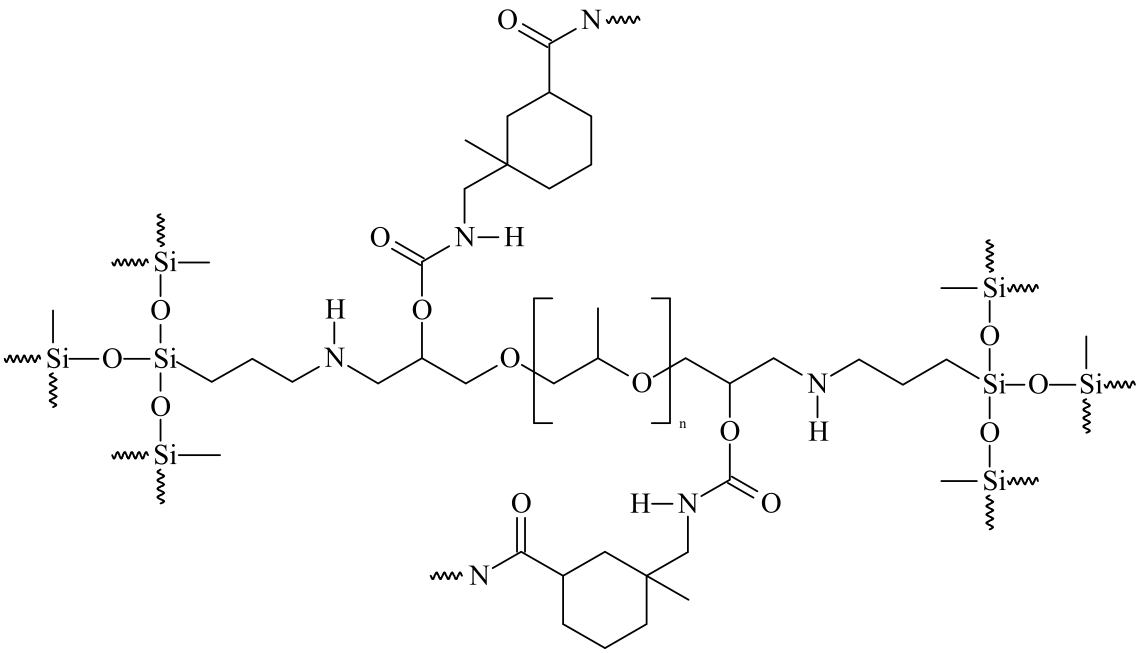

Figure 1. Proposed chemical structure of the prepared hybrid coating C4.

The FTIR spectrum of coating C4 (Figure 2) showed a strong absorption peak at 1075 cm^{-1} that corresponds to Si-O-Si which confirms the condensation reaction between the silanol groups. The disappearance of absorption peak at 905 cm^{-1} for epoxy group indicated that the epoxy groups had reacted with APTMS and is now attached to the silica by a chemical bond.[23] The formation of the urethane moiety can be proved from the absorption peak at 1707 cm^{-1} and the disappearing of any absorption peaks at 2270 cm^{-1} corresponds to unreacted isocyanates.[24] The existence of absorption band at 3346 cm^{-1} indicates that not all the -OH groups were consumed during the condensation reaction or it may corresponds to the -NH groups. The peaks in the range 1400-1600 cm^{-1} correspond to the combination of bending vibration of N-H bond and stretching vibration of C-N bond. The FTIR spectra of all other coatings (Supporting Information) showed also the above characteristic absorption peaks but with clear shift in their corresponding frequency values. The shifts in the IR frequencies of carbonyl groups to lower numbers in all other coatings could be attributed to the Hydrogen bonding interaction for these groups with -NH and -OH groups,[25] or to the presence of Urea content in the coating's composition.[26] More absorption peaks can be observed in the FTIR spectrum of coating C2 that could be assigned to the silane precursor GPTMS in the coating formulation.

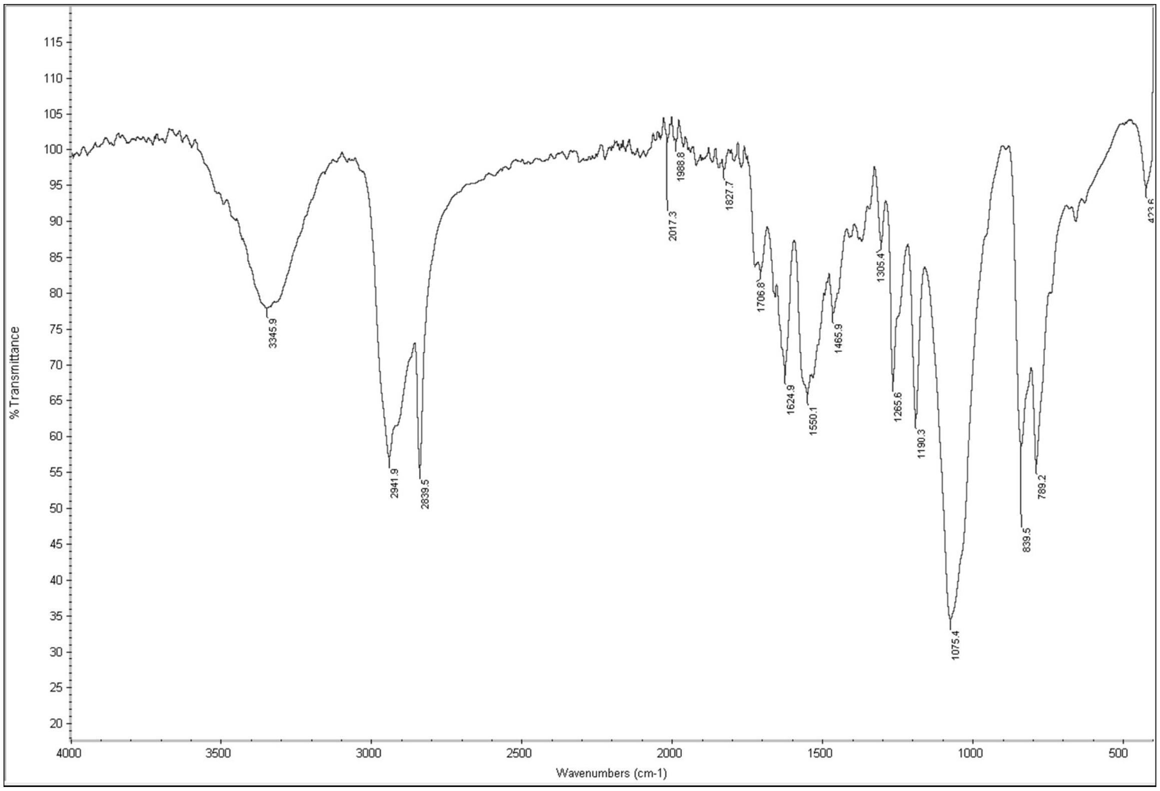

Figure 2. FTIR spectrum for the hybrid coating C4.

Furthermore, the same compound (C4) was subjected to ^{1}H-NMR and carbon-13 nuclear magnetic resonance (^{13}C-NMR) analyses. ^{1}H-NMR spectrum (Figure 3) showed the disappearance of the chemical shift at 2.60 ppm which is assigned for the proton of the carbon in the oxirane rings. This confirms the occurrence of the reaction between the epoxide groups in DER736 and the amino group in APTMS. This was also confirmed by observing that the chemical shift of the proton in the NCH_2 group in the APTMS monomer (2.02 ppm) has now shifted downfield in C4 (2.74 ppm). The presence of small signal at 2.99 ppm in C4 indicates that not all OMe groups in APTMS were hydrolyzed during the sol-gel reaction. The corresponding ^{13}C-NMR spectrum of C4 is illustrated in Figure 4. The spectrum shows the carbon in $SiCH_2$ has shifted upfield from 5.8 ppm in the APTMS monomer to -7.2 and -9.1 ppm in C4.[27] The spectrum shows also the appearance of two peaks at 54.7 and 63.8 ppm resulted from the opening of the epoxide ring after crosslinking with APTMS. The four peaks in the range of 156.3 to 159.1 ppm correspond to different urea/urethane carbonyls in C4 confirming the reaction of the isocyanate groups (no peaks corresponding to the isocyanate carbons is shown in the range 122.0 to 124.0 ppm) in IPDI. NMR spectra of the different coatings and the precursors were given in the supporting information.

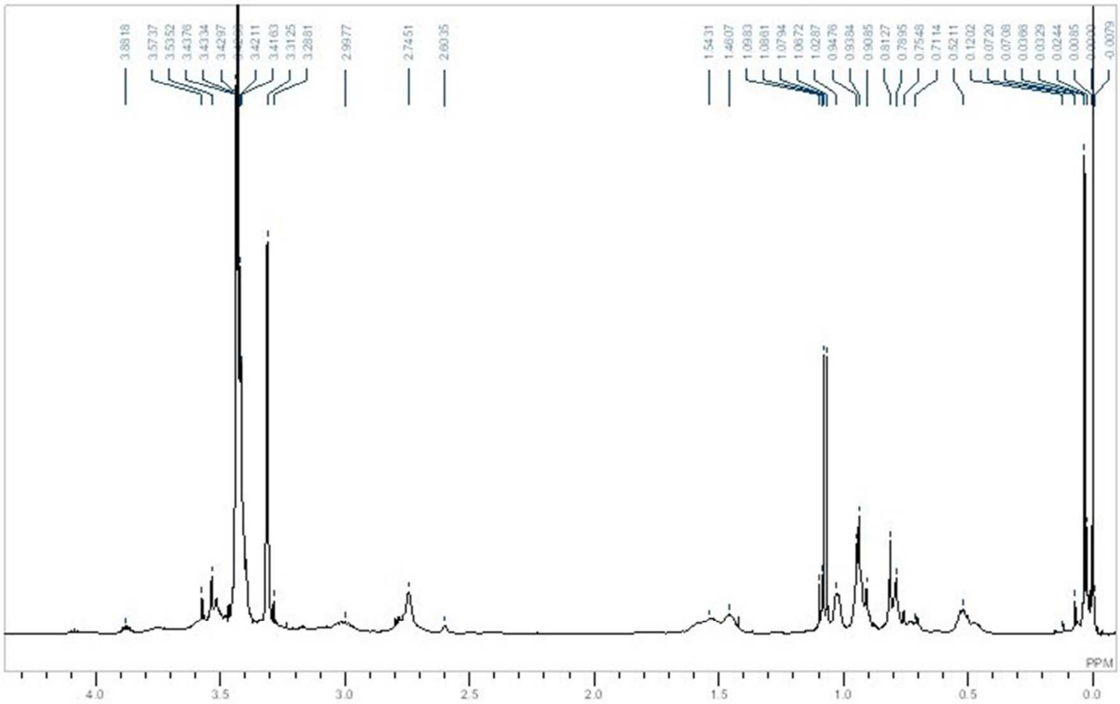

Figure 3. ^{1}H-NMR spectrum for the hybrid coating C4.

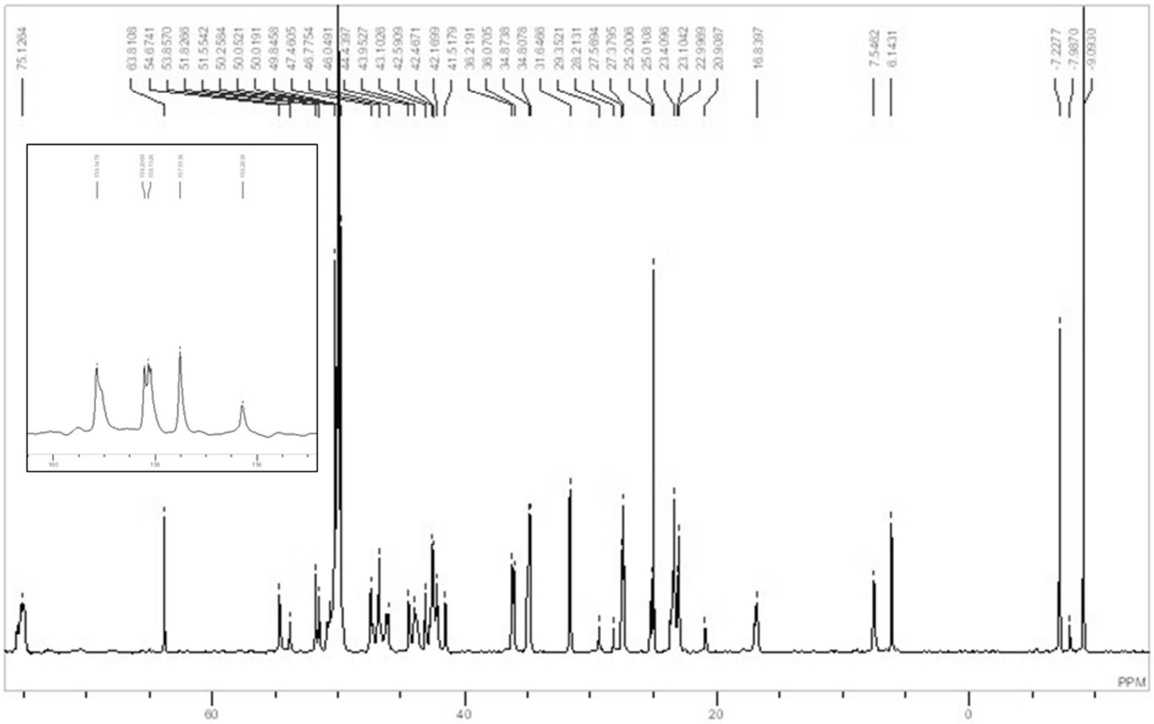

Figure 4. ^{13}C-NMR spectrum for the hybrid coating C4.

Physical Appearance of Cured Coatings

After application and curing of coatings, the samples appeared very similar and showed no visible signs of corrosion or cracks (Fig. 5). The difference in the original color of the prepared coatings before application on steel panels (Colorless for C1, C3 and C5; Pale yellow for C2 and C4) causes the slight change in the color of the cured coated samples. The cured samples subjected then to different thermal, electrochemical, morphological and hardness testing. It is worth mentioning here that the following properties of each individual coating are the average properties of all different polymeric segments forming that coating's formulation.

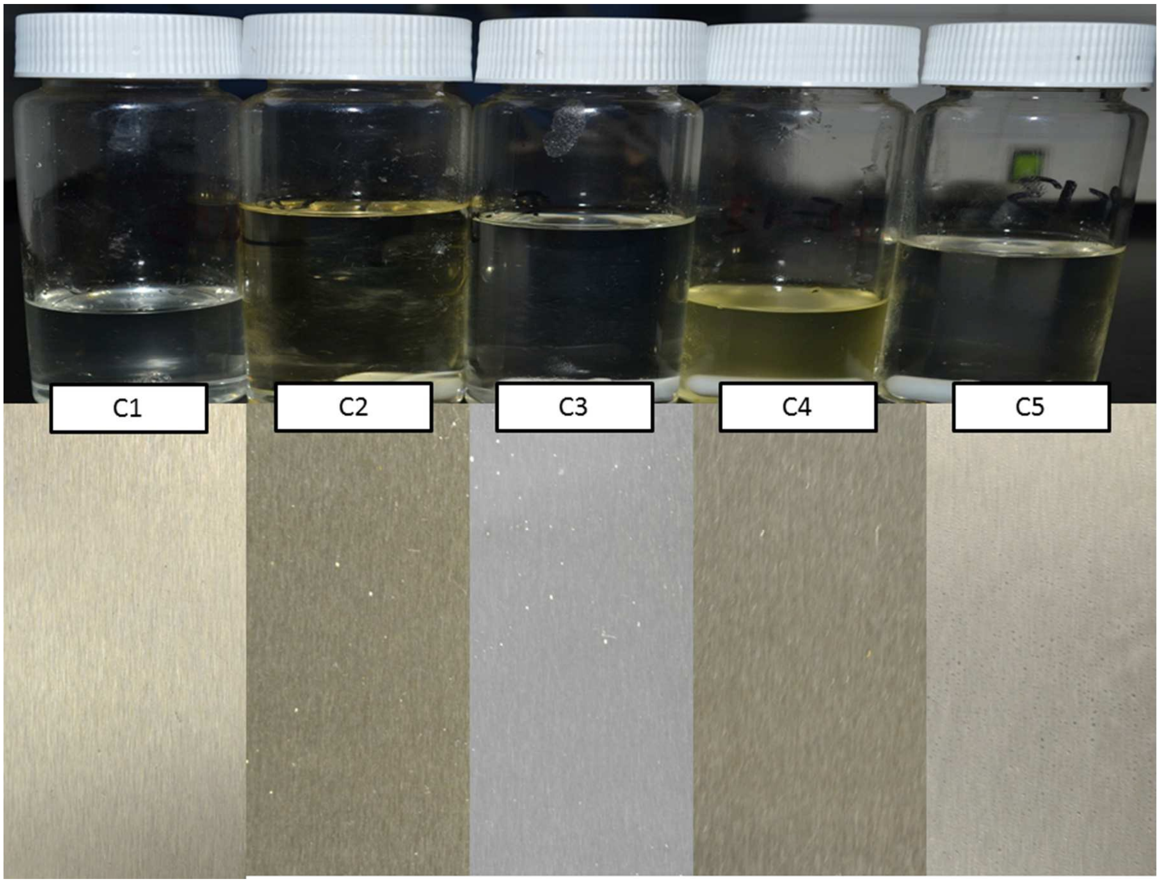

Figure 5. Coated samples after curing.

Thermal Analysis

The thermal stability of the prepared organic-inorganic hybrid coatings were determined by using TGA analysis. The thermograms for different hybrid coatings are given in Figure 6. The results revealed that all prepared coatings were characterized by high thermal stability, except for coating C5, which indicated weak crosslinking density for this coating.

The weight losses for C5 take place at three steps: The first step with gradual weight loss from room temperature to around 325 °C is due to the evaporation of physically absorbed solvent and residual monomers, the second weight loss in the range of 325 ~ 510 °C is ascribed to the decomposition of polymer, the third minor weight loss at 510 ~ 700 °C may be caused by the partial decomposition of silica bonded or entrapped polymeric segments.[28] The weight loss pattern of all other coatings are relatively similar to C5 but with small changes in the corresponding intervals of temperatures and significant lower char yields.

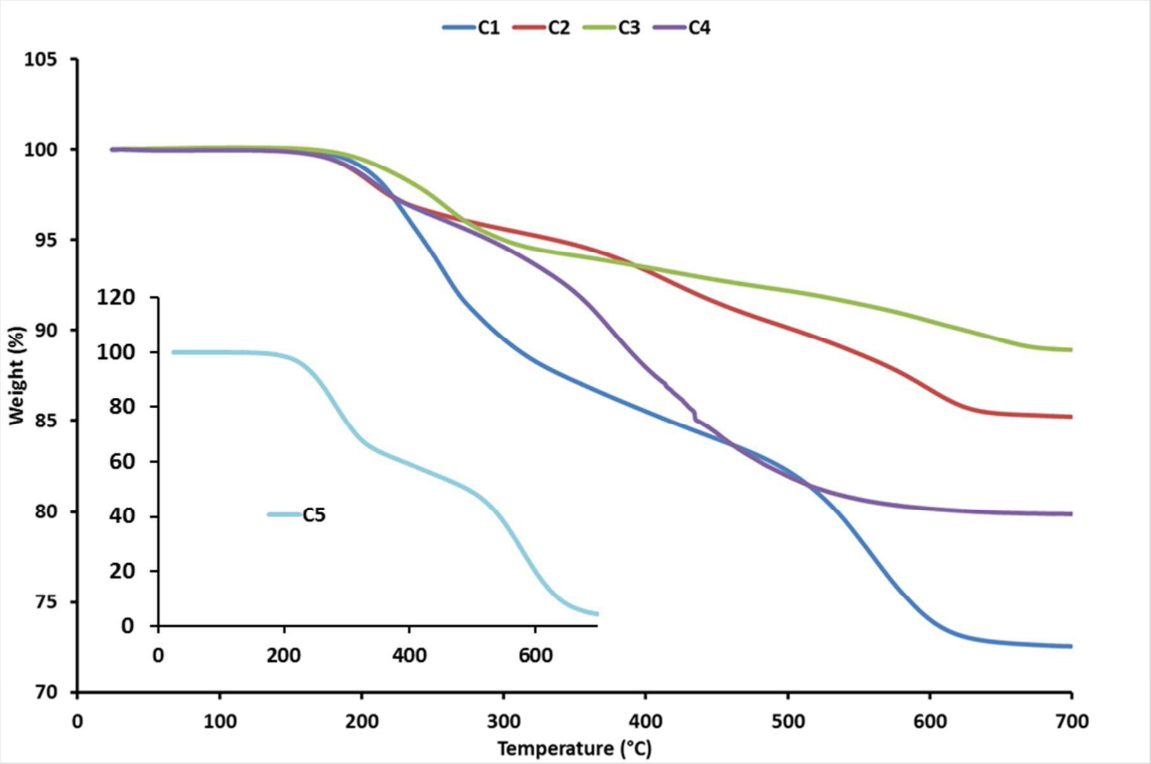

Figure 6. TGA analysis for the hybrid coatings.

Electrochemical Impedance Studies

The protective character of the newly prepared hybrid sol-gel coatings was determined using electrochemical measurements, and in particular the EIS technique. The most outstanding and well-known advantage of this technique is the possible continuous monitoring of the progress of corrosion, with instantaneous corrosion rate measurements, and it can provide information on the reactions mechanisms of the electrochemical deterioration.[29] The impedance response of the system consists of the sol-gel layer, the activity at the substrate/coating interface, and the corrosion process that might take place.

The open-circuit impedances of the hybrid sol-gel coated mild steel substrate were traced over 240 h after immersing them continuously into 3.5 wt% NaCl solution.

The electrochemical impedance Bode spectra for all the coatings after 24 and 240 hours of continuous immersion in 3.5 wt% NaCl electrolyte is shown in Figure 7(a and b). EIS data clearly indicated that all coatings (except C2) provided excellent barrier protection properties for the steel surface at initial immersion time in NaCl solution. Initially, the C3 coated sample showed the highest impedance value (9.2 x 10^7 Ω cm^2) among all the coated samples (Figure 7a). Interestingly, only sample C4 showed no significant change in its impedance value (8.2 x 10^6 Ω cm^2) after 240 hours of immersion, indicating a minor loss of the corrosion protection properties of this coating. The impedance values for the other coatings were in the following order: C3 (4.5 x 10^5 Ω cm^2) > C1 (2.3 x 10^5 Ω cm^2) > C2 (8.8 x 10^4 Ω cm^2) > C5 (1.0 x 10^4 Ω cm^2) (Figure 7b). The low impedance value for coating C5 at longer immersion times in NaCl revealed the failure of this coating in protecting steel surface from corrosion.

Figure 8 represents the EIS Nyquist spectra of the hybrid sol-gel mild steel coated samples after 24 and 240 hours of immersion in the electrolyte solution. Nyquist plot of the coated sample C3 after 24 hours of immersion indicated the presence of only one capacitive arc, which implied that the coating acts as intact capacitor prohibiting the permeation of corrosive species such as water, oxygen, and other ions towards the surface of the metal substrate (Figure 8a). The Figure showed that the impedance properties of this coating are higher than all other samples. The Nyquist plots of other coated samples showed two-time constant semicircles with depressed and full capacitive first loop for each coating at higher frequencies. Larger diameters of Nyquist semi-circles are attributed of higher corrosion resistance coatings. At prolonged immersion periods, the nyquist plots (Figure 8b) showed that the highest corrosion resistance is now for C4. For samples C1-C3 and C5, there is a presence of a semicircle at low frequencies in the nyquist plot, suggesting the onset of electrochemical reactions at the metal/coating interface.[4] The relatively high resistances of the C4 coating and its stability over the long immersion period confirmed its barrier protection properties.

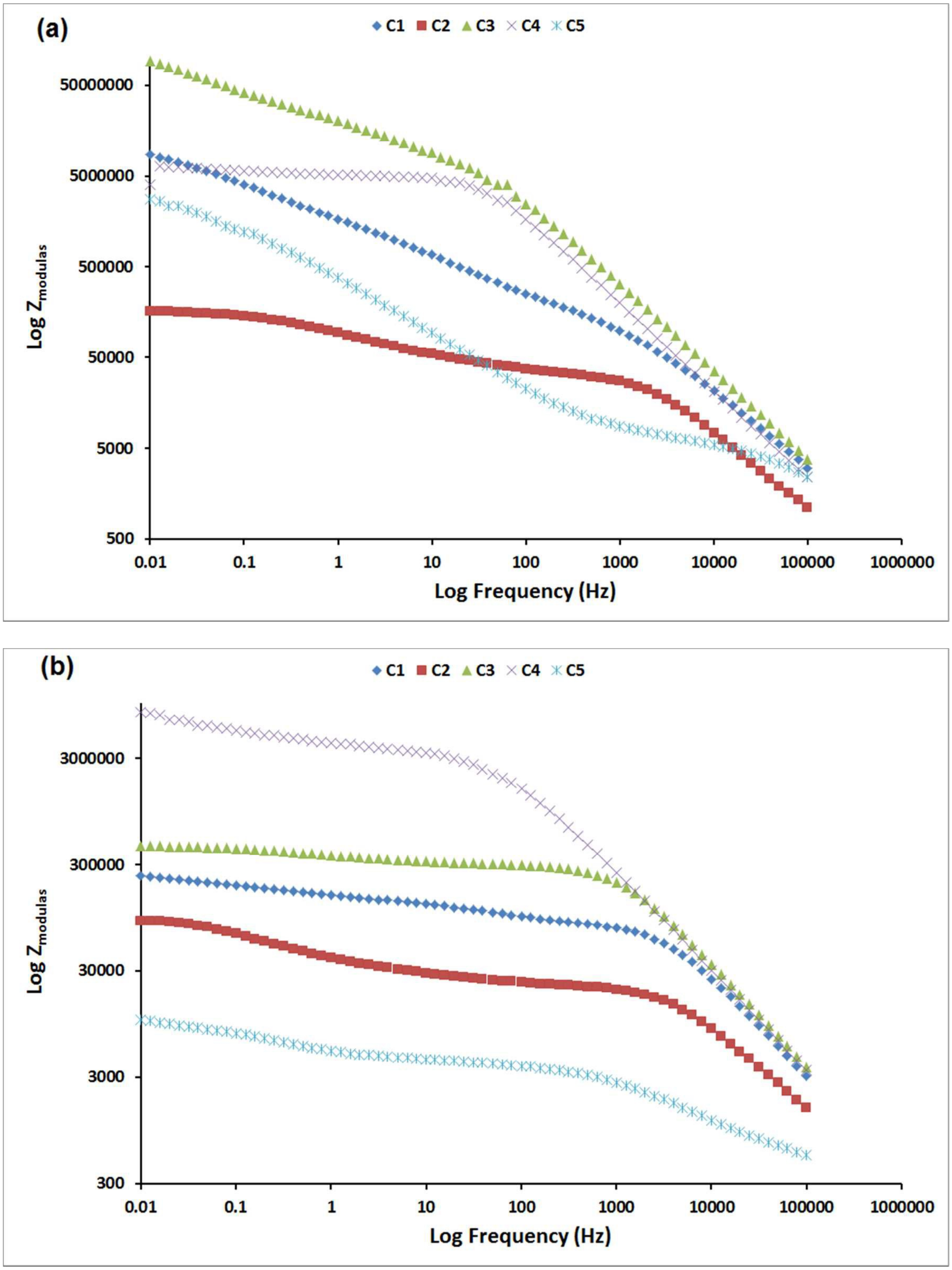

Figure 7. Bode plots of the hybrid coated mild steel samples after (a) 24 and (b) 240 hours immersion in 3.5 wt% NaCl solution.

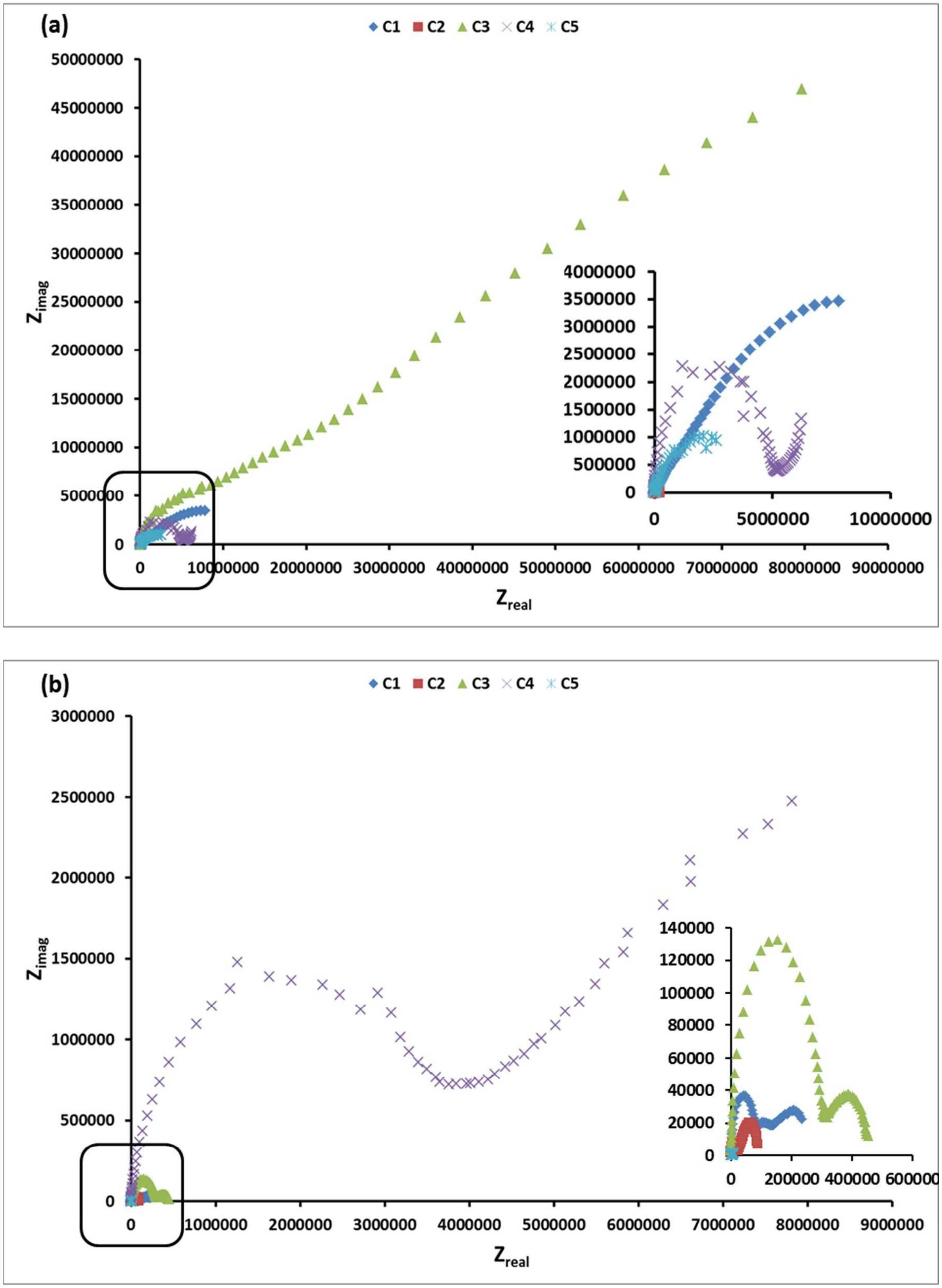

Figure 8. Nyquist plots of the hybrid coated mild steel samples after (a) 24 and (b) 240 hours immersion in 3.5 wt% NaCl solution.

Potentiodynamic Polarization Tests

The polarization curves of the hybrid coated mild steel samples after 240 h immersion in 3.5 wt% NaCl solution are shown in Figure 9, and the electrochemical characteristics derived from these curves are listed in Table 2. The results showed that the I_{corr} of sample C4 is much less than all other samples, which confirmed the excellent barrier properties of this hybrid coating. This result reveals that there is a greatest crosslinked structure of C4 among all other coatings.[30] Considering the data displayed in Table 2, it was evident that the results of polarization tests were consistent with those of impedance measurements in which sample C4 showed the best corrosion protection performance on mild steel substrate, while sample C5 showed the poorest performance. The poor performance of C5 can be attributed to the formation of a less dense and porous coating's film on the surface of steel.

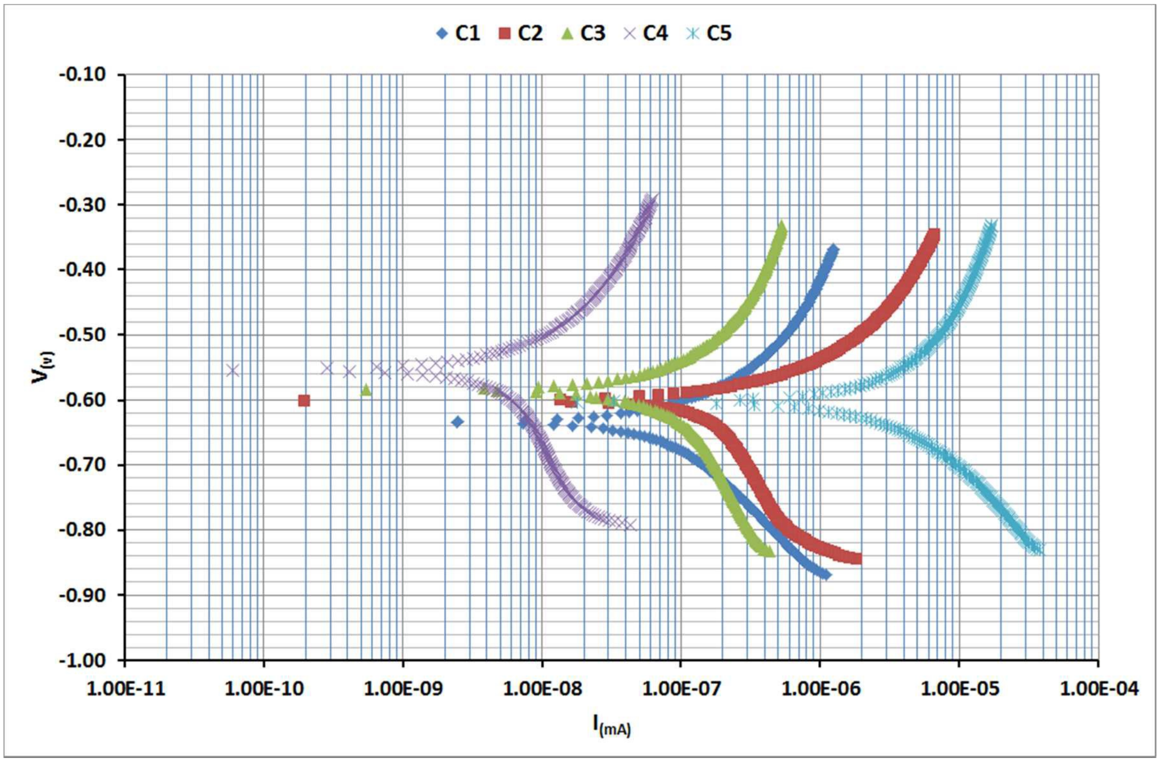

Figure 9. DC polarization scans of the hybrid coated mild steel samples after 240 h immersion in 3.5 wt% NaCl solution.

Table 2. Electrochemical characteristics of the hybrid coated mild steel samples after 240 h immersion in 3.5 wt% NaCl solution

Sample	C1	C2	C3	C4	C5

E_{corr} (mV)	-633	-6.01	-584	-553	-603
I_{corr} (A/cm^2)	1.04×10^{-7}	2.55×10^{-7}	1.19×10^{-7}	1.94×10^{-8}	1.42×10^{-6}

Morphological Studies

Figure 10 shows scanning electron micrographs of the top surface of the fractured surfaces of C1-C5 samples, respectively. The EDX analysis confirmed the application of the coatings on the substrate due to the appearance of carbon, oxygen and silicon elements. We observed a smooth and featureless morphology for C3 and C4. The surface of samples C1 and C5 appeared rough with small cracks and some NaCl salt precipitation on them. They appeared also to consist of two or more phases that are dispersed in the coating matrix, indicating the occurrence of different competitive polymeric reactions during the preparation of these coatings. The surface of sample C2 showed the shape of regular non-porous coatings with the presence of some coating particles that did not crosslinked with the bulk of the coating and existed on the surface of the coating layer already attached to the metal. The nature of these particles was elucidated using single point EDS analysis of the coated sample (Supporting Information). The above results are in full agreement with electrochemical tests which proved the C4 sample to have the best barrier properties among all other prepared coatings.

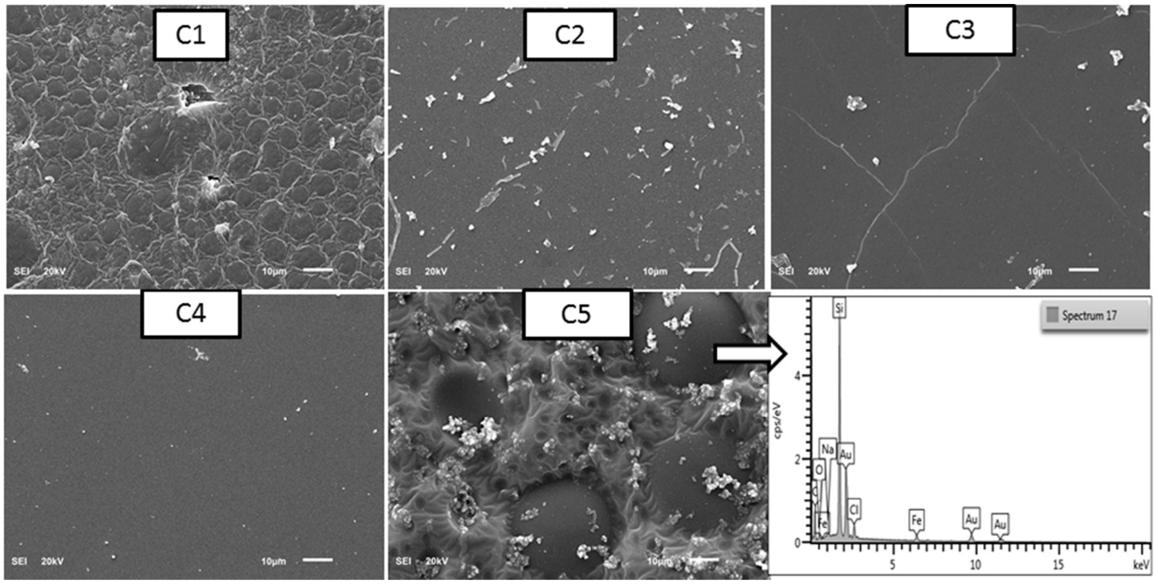

Figure 10. SEM micrograph of the top surface of hybrid coated samples immersed in 3.5 wt% NaCl for 10 days (insert: EDS analysis on a single-point on the surface of the sample C5)

Figure 11 shows the typical SEM photographs of cross sections of the hybrid sol-gel coated mild steel samples. It was observed that the coatings are perfectly bonded with no sign of any defects.

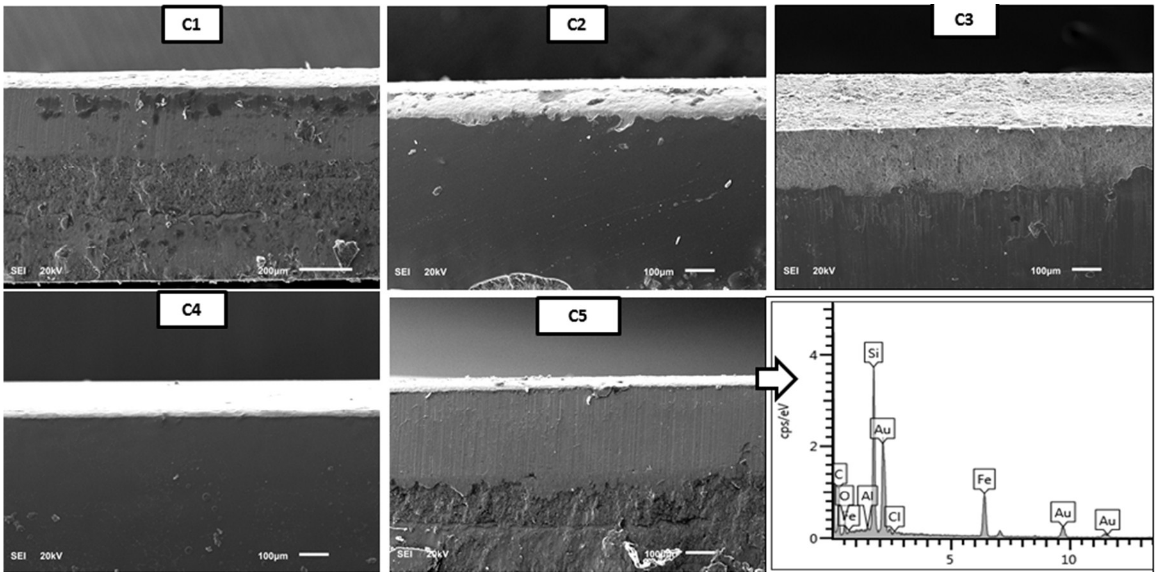

Figure 11. SEM image of a cross-section of hybrid coatings (insert: EDS analysis on a single-point on sample C5)

The photo digital imaging of all coated samples after immersing them continuously for 10 days in 3.5 wt% NaCl solution (Figure 12) confirmed the conclusion drawn from the electrochemical data. Both samples C1 and C5 showed signs of advance corrosion on their surfaces, while samples C2 and C3 showed the presence of some salt aggregates adsorbed on their surfaces. The surface of sample C4 remained intact with no sign of corrosion or coating delamination.

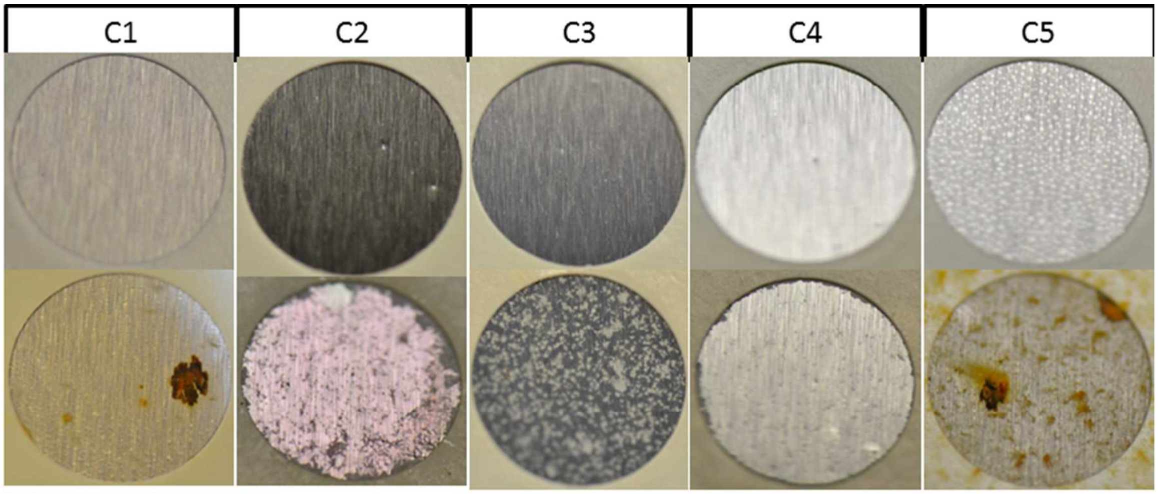

Figure 12. Sections of the panels shown in Figure 5 before and after immersion in 3.5 wt% NaCl for 10 days.

Contact Angle Measurements

Contact angle is an important parameter to evaluate the surface of hybrid coatings. The contact angle values for the hybrid coatings before and after immersion in 3.5 wt% NaCl for 10 days are shown in Figure 13. Although the surface of the coated sample C4 has the lowest hydrophobic character (due to the less organic functionalities in this coating) among all other coated samples, it showed less wetting (following the drop in contact angle values before and after immersion) behavior comparing to the other samples, which explain also the interesting anticorrosive property of this coating. The loss in the hydrophobicity of surfaces is an indication for wetting the hybrid coatings with electrolyte solution which leads eventually to the onset of corrosion.[31]

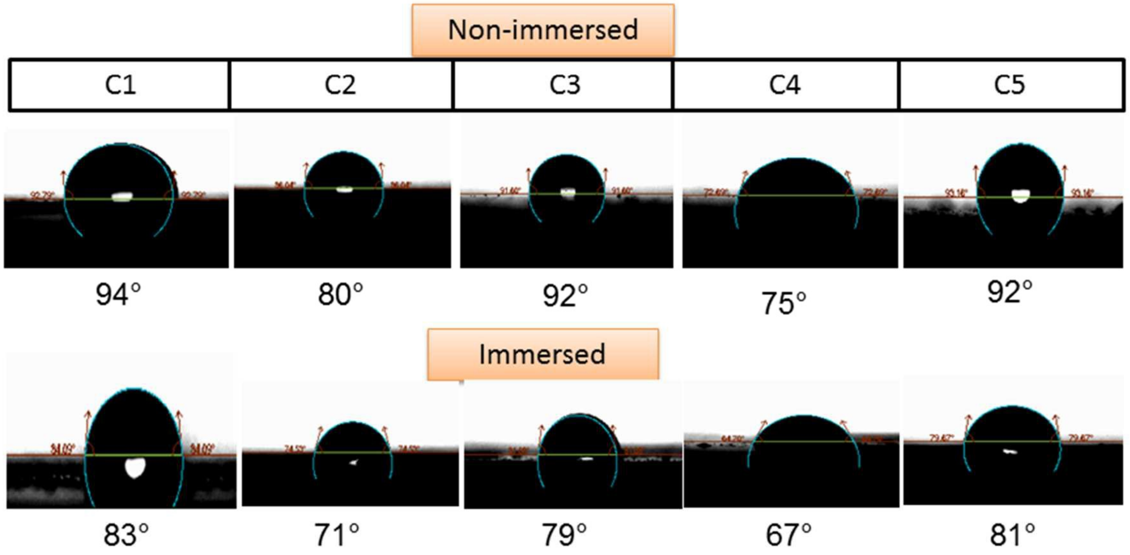

Figure 13. The contact angle for the hybrid coatings before (Non-immersed) and after (Immersed) immersion in 3.5 wt% NaCl for 10 days.

Hardness Test

Nanoindentation analysis was used to evaluate the hardness of the prepared coatings and obtained results are presented in Table 3. The high hardness of sample C4 revealed the existence of a higher sol-gel density in this coating comparing to other coatings,[32] which supported and explained the interesting anticorrosive properties of this coating. The similarity in the profile of both mechanical and the anticorrosion properties was also visible with other coatings except for sample C5, where the hardness value of this coating was affected by the hardness properties from the steel substrate.[33] This interference can be attributed to the thin film this coating formed on the steel surface.

Table 3. Nanoindentation Hardness and Thickness of the hybrid coatings

Sample	Nanoindentation hardness (GPa)*	Contact Depth (mm)*	Thickness (mm)**
C1	0.55 ± 0.01	14 ± 0.3	74
C2	0.23 ± 0.01	11 ± 0.5	115
C3	1.35 ± 0.06	11 ± 0.1	140
C4	3.47 ± 0.03	4 ± 0.1	122
C5	7.36 ± 1.5	7 ± 1.7	40

* Determined using a load of 50 mN (average of 4 measurements).

** Obtained from cross-sectional SEM analyses.

Adhesion Test

The adhesion capacity of all the coatings was measured using the pull-off hydraulic adhesion tester. Results in Figure 14 indicated clearly the superior adhesion strength of C4 as compared to other coatings. This can be explained by the availability of more free Si-OH groups in this coating to bond to steel surface.[34]

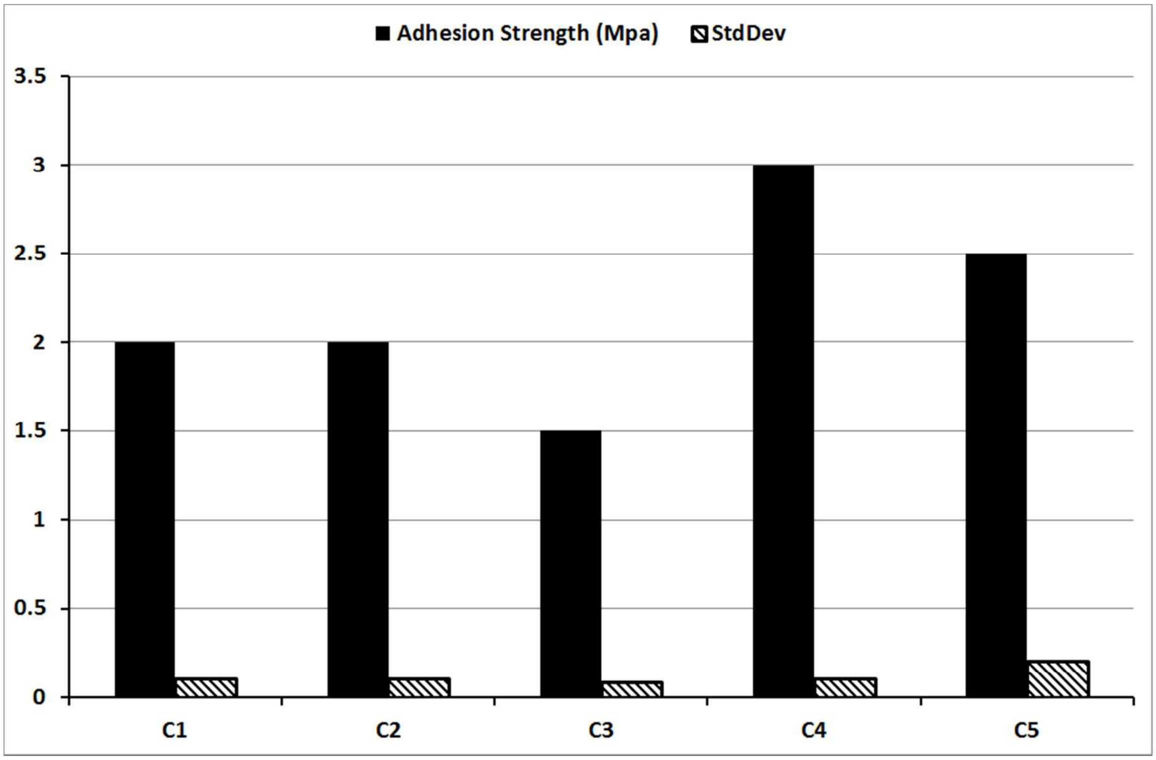

Figure 14. Adhesion strengths (in Mpa, average of 3 measurements) of hybrid coatings.

The superior anticorrosive, hardness and adhesion properties of C4 can be attributed to the powerful ability of the APTMS crosslinker to contribute effectively and simultaneously in both the coupling and the hydrolysis/polycondensation reactions. This led ultimately to the production of a homogeneous coating with high crosslink density, while the other two considered aminosilanes in this study were characterized by a low crosslink density that provides pathways for the diffusion of corrosive species to the coating/metal interface.

In order to explore the protection performance of C4 in other aggressive media and at longer immersion time, completely cured C4 coated steel panels were immersed continuously in 3.5 wt% NaCl, 2M H_2SO_4 and 1M HCl electrolytes for two weeks. Photodigital images of the immersed panels (Figure 15) showed clearly that the two coated panels immersed in NaCl and SO_4^{2-} electrolytes (Figure 15a and b, respectively) remained intact indicating an excellent corrosion protection performance of C4 on steel surface in these two testing media. Opposite behavior was observed with the sample immersed in the HCl solution (Figure 15c) where the steel surface was massively suffered from the occurrence of both general corrosion and delamination of coating behaviors. The promising corrosion protection result obtained with C4 in SO_4^{2-}

encouraged us to initiate a full study on investigating the protection performance of all the other coatings we are reporting in this study under the corrosive sulfate medium.

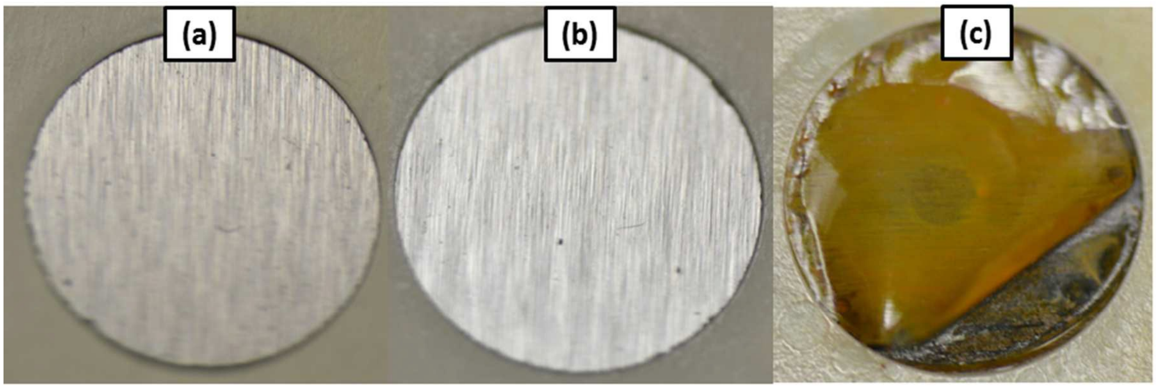

Figure 15. C4 coated steel panels after two weeks of immersion in (a) 3.5 wt% NaCl, (b) 2M H_2SO_4 and (c) 1M HCl solutions.

CONCLUSIONS

A series of siliconized epoxy hybrid organic-inorganic coatings were prepared, coated on mild steel panels, and subjected to structure elucidation, heat resistance, contact angle, nanoindentation hardness, pull-off adhesion and electrochemical corrosion studies. The properties of the hybrid coatings varied with type of the aminosilane coupling agent and the trialkoxysilane components. EIS and polarization analyses results on coated samples indicated excellent anticorrosion barrier properties for the hybrid coating prepared starting from the aminosilane APTMS (C4). SEM analyses complemented the electrochemical experiments and revealed no cracks and defects in C4 and the existence of inhomogeneity and defects in all other coatings. All coatings (except C5) present good heat resistance, adhesion and hardness. The surfaces of the prepared coatings were having a slight hydrophobic character. All of the above properties for the newly-prepared coatings provided us with promising alternative substituents for the conventional chromate conversion coatings.

ACKNOWELDGMENT

We thank King Fahd University of Petroleum and Minerals (KFUPM Saudi Arabia) for providing all support to this project. This project has been funded by King Fahd University of Petroleum and Minerals under project no. IN131061.

REFERENCES

1. J. H. Potgieter, P. A. Olubambi, L. Cornish, C. N. Machio, E. S. M. Sherif, Influence of nickel additions on the corrosion behaviour of low nitrogen 22% Cr series duplex stainless steels, *Corrosion Science*, 2008, **50**, 2572–2579.
2. Min Qian, Andrew Mcintosh Soutar, Xiu Hui Tan, Xian Ting Zeng and Sudesh L. Wijesinghe, Two-part epoxy-siloxane hybrid corrosion protection coatings for carbon steel, *Thin Solid Films*, 2009, **517**, 5237–5242.
3. C. Chang, C. Wang, C. Wu, S. Liu, F. Mai, Using ToF-SIMS and EIS to evaluate green pretreatment reagent: Corrosion protection of aluminum alloy by silica/zirconium/cerium hybrid coating, *J. Appl. Surf. Sci*., 2008, **255**, 1531-1533.
4. R. Suleiman, M. Mizanurrahman, N. Alfaifi, B. El Ali, R. Akid, Corrosion resistance properties of hybrid organic-inorganic epoxy-amino functionalized polysiloxane based coatings on mild steel in 3.5% NaCl solution, *Corrosion Engineering, Science and Technology*, 2013, **48**, 525-529.
5. R. Suleiman, M. Khaled, H. Wang, J. Gittens, T. Smith, R. Akid, B. El Ali, A. Khalil. A comparison of selected inhibitor doped sol-gel coating systems for the protection of mild steel. *Corrosion Engineering, Science and Technology*, 2014, **49**, 189-196.
6. R. Suleiman, Corrosion Protective Performance of Epoxy - Amino Branched Polydimethylsiloxane Hybrid Coatings on Mild Steel, *Anti-Corrosion Methods and Materials*, 2014, **61**, 423-430.
7. M. Fedel, M. Olivier, M. Poelman, F. Deflorian, S. Rossi, M.-E. Druart, Corrosion protection properties of silane pre-treated powder coated galvanized steel, *Progress in Organic Coatings*, 2009, **66**, 118–128.
8. S. K. Poznyak, M. L. Zheludkevich, D. Raps, F. Gammel, K. A. Yasakau, M. G. S. Ferreira, Preparation and corrosion protective properties of nanostructured titania-containing hybrid sol–gel coatings on AA2024, *Progress in Organic Coatings*, 2008, **62**, 226–235.
9. V. Moutarlier, B. Neveu, M. P. Gigandet, Evolution of corrosion protection for sol–gel coatings doped with inorganic inhibitors, *Surface and Coatings Technology*, 2008, **202**, 2052–2058.
10. S. V. Lamaka, M. F. Montemor, A. F. Galio, M. L. Zheludkevich, C. Trindade, L. F. Dick, M. G. S. Ferreira, Novel hybrid sol–gel coatings for corrosion protection of AZ31B magnesium alloy, *Electrochim. Acta*, 2008, **53**, 4773–4783.
11. M. W. Daniels and L. F. Francis, Silane adsorption behavior, microstructure, and properties of glycidoxypropyltrimethoxysilane-modified colloidal silica coatings, *J. Colloid. Inter. Sci.*, 1998, **205**, 191-200.

12. M. W. Daniels and L. F. Francis, Effect of Curing Strategies on Porosity in Silanemodified Silica Colloidal Coatings, *Mater. Res. Proc. Res. Soc.*, 1999, **576**, 313-317.

13. S. H. Cho, S. R. White, P. V. Braun, Room-temperature polydimethylsiloxane-based self-healing polymers, *Chem. Mater.*, 2012, **24**, 4209-4214.

14. M. Y. Sho, H. Kwon, Comparison of surface modification with amino terminated polydimethylsiloxane and amino branched polydimethylsiloxane on the corrosion protection of epoxy coating, *Corrosion Science*, 2009, **51**, 650-657.

15. H. Wang, R. Akid, A room temperature cured sol–gel anticorrosion pre-treatment for Al 2024-T3 alloys, *Corrosion Science*, 2007, **49**, 4491-4503.

16. A. Bandyopadhyay, A. R. Bhowmick, M. De Sarkar, Synthesis and characterization of acrylic rubber/silica hybrid composites prepared by sol-gel technique, *Journal of Applied Polymer Science*, 2004, **93**, 2579–2589.

17. D. K. Chattopadhyay, D. C. Webster, Hybrid coatings from novel silane-modified glycidyl carbamate resins and amine crosslinkers, *Progress in Organic Coatings*, 2009, **66**, 73–85.

18. A. J. Vreugdenhil, V. J. Gelling, M. E. Woods, J. R. Schmelz, B. P. Enderson, The role of crosslinkers in epoxy–amine crosslinked silicon sol–gel barrier protection coatings, *Thin Solid Films*, 2008, **517**, 538–543.

19. P. Gupta, M. Bajpai, Development of Siliconized Epoxy Resins and Their Application as Anticorrosive Coatings, *Advances in Chemical Engineering and Science*, 2011, **1**, 133-139.

20. P. Bajpai and M. Bajpai, Development of a high performance hybrid epoxy silicone resin for coatings, *Pigment & Resin Technology*, 2010. **39**, 96-100.

21. S. K. Rath, J. G. Chavan, S. Sasane, Alips Srivastava, M. Patri, A. B. Samui, B. C. Chakraborty, S. N. Sawant, Coatings of PDMS-modified epoxy via urethane linkage: Segmental correlation length, phase morphology, thermomechanical and surface behavior, *Progress in Organic Coatings*, 2009, **65**, 366–374.

22. A. L. K. Tan, A. M. Soutar, Hybrid Sol-gel Coatings for Corrosion Protection of Copper, *Thin Solid Films*, 2008, **516**, 5706–5709.

23. Weili Li, Dong Huang, XinYu Xing, Jijun Tang, Yujin Xing, Xiujuan Li, Jide Zhang, Study the Factors Affecting the Performance of Organic–Inorganic Hybrid Coatings, *Journal of Applied Polymer Science*, 2014, DOI: 10.1002/APP.41010.

24. H. J. Naghash, I. Mohammadidehcheshmeh, M. Mehrnia, Synthesis and characterization of a novel hydroxy terminated polydimethylsiloxane and its application in the waterborne polysiloxane–urethane dispersion for potential marine coatings, *Polym. Adv. Technol.*, 2013, **24**, 307–317.

25. E. Yilgör, E. Burgaz, E. Yurtsever, İ. Yilgör, Comparison of hydrogen bonding in polydimethylsiloxane and polyether based urethane and urea copolymers, *Polymer*, 2000, **41**, 849–857.

26. Shi-Kwun Wang, Chong Sook Paik Sung, Fluorescence and IR Characterization of Cure in Polyurea, Polyurethane, and Polyurethane-Urea, *Macromolecules*, 2002, **35**, 883-888.
27. S. Sobhani, A. Jannesari, S. Bastani, Effect of Molecular Weight and Content of PDMS on Morphology and Properties of Silicone-Modified Epoxy Resin, *Journal of Applied Polymer Science*, 2012, **123**, 162-178.
28. Yong-Chun Chen, Shu-Xue Zjou, Hai-Hua Yang and Li-Min Wu, Interaction and Microstructure of Polyurethane/Silica Hybrid Films Prepared by Sol-Gel Process, *Journal of Sol-Gel Science and Technology*, 2006, **37**, 39–47.
29. N. P. Tavandashti, S. Sanjabi, T. Shahrabi, Evolution of corrosion protection performance of hybrid silica based sol–gel nanocoatings by doping inorganic inhibitor, *Materials and Corrosion*, 2011, **62**, 411-415.
30. K. H. Wu, C. M. Chao, T. F. Yeh, T. C. Chang, Thermal stability and corrosion resistance of polysiloxane coatings on 2024-T3 and 6061-T6 aluminum alloy, *Surface & Coating Technology*, 2007, **201**, 5782-5788.
31. H. R. Jeon, J. H. Park, M. Y. Shon, Corrosion protection by epoxy coating containingmulti-walled carbonnanotubes. *Journal of Industrial and Engineering Chemistry*, 2013, 19, 849–853.
32. S. Frings, H. A.Meinema, C. F. Van Nostrum, R. Van der Linde, Organic-inorganic hybrid coatings for coil coating application based on polyester and tetraethoxysilane, *Progress in Organic Coatings*, 1998, **33**, 126–130.
33. H. Ichimura, I. Ando, Mechanical properties of arc-evaporated CrN coatings: Part I - nanoindentation hardness and elastic modulus, *Surface and Coatings Technology*, 2001, **145**, 88-93.
34. M.-C. Brochier Salon and M. N. Belgacem. Competition between hydrolysis and condensation reactions of trialkoxysilanes, as a function of the amount of water and the nature of the organic group. *Colloid Surface A*, 2010, **366**, 147–154.